ABSTRACT

In this study, we plan to find dissimilarities between normal cells and cancerous cells, through investigating HiC contact maps. We suspect that there are systematic differences between how chromosomes are structured between normal cells and cancerous cells. we Ideally, it is desirable to compare 3D structures of cell in order to make such comparisons. However, the main challenge that we face is that 3D structure of a cell is not readily available. Based on (1), fluorescence in situ hybridizaiton (FISH) is used for investigating 3D configuration of chromosomes. However, this method can only be used locally and cannot map the whole structure of the chromosomes. In orther to find dissimilarities in the 3D structure of chromosomes, we used HiC dataset. The HiC method, which was developed by (2), captures interactions between chromosomal fragments in kilobase resolution. Based on HiC data, an *interaction frequency (IF)* matrix can be developed between *loci* at a desired resolution. A cell IF_{ij} in an interaction frequency matrix captures the number of interaction detected in HiC dataset between locus i and locus j in the genome. An interaction matrix can be used to develop both inter- and intra-chromosomal interaction matrices. We believe differences in interaction matrices can be found between normal cells and cancerous ones.

INTRODUCTION

Graphlet comparison is a novel method used to compare large networks in order to find local similarities in them. Authors of (3) provide a new measure of PPI network comparison based on 73 constraints. This is used in order to compare two large networks in order to detect similarities.

(4) provide heuristics to compare two nodes based on some feature (or signature) vectors, which is a 73-dimensional vector $\mathbf{s}^T = [s_0, s_2, ..., s_{72}]$ where s_i denotes the number of nodes in the network that are part of an orbit i.
Important Result: Proteins with similar surroundings perform similar functions.

In (5), the same author investigates cancer-causing genes to find similarities in their signatures. After clustering the genes based on *signature similarity* criteria, some clusters contain a lot of cancerous genes. They use 4 different clustering methods with varying parameters to cluster the proteins. They then predict the cancer-relatedness of a protein i using an enrichment criteria $\frac{k}{|C_i|}$ where C_i is the cluster where protein i belongs and k is the number of cancer-causing proteins in C_i and $|C_i|$ is the size of C_i.

The authors of (6) generalized the idea of graphlets to ordered graphs were the nodes are labeled in ascending order. As can be viewed, there are a total of 14 orbits for graphlets of size 2 and 3 since the label of graphlets is also included in toplogy. In the new definition, d_v^i denotes the number of orbit i touches node v. Each node, is then assigned a vector of length 14 [1] $(d_v^1, d_v^2, ..., d_v^{14})$ and similarity of two nodes in two contact maps can be compared by how geometrically close their corresponding vectors are.

[1] number of orbits in graphlets of size 2 and 3

MATERIALS AND METHODS

Thresholding contact maps

In order to be able to extract graphlets, HiC contact maps should be modeled as unweighted graphs where the nodes represent the loci and an edge between two nodes represent a *significant* interaction between the loci the nodes represent.

Thresholding is achieved by thresholding the contact maps. The result of the thresholding procedure would be a binary matrix which also can serve as an adjacency matrix for an unweighted, undirected graph. The graph can then be used for orbit extraction.

In order to go about the process of thresholding, it is necessary to make sure that both global and local features are maintained. We could consider thresholding the contact maps by simply setting values above a fixed value to one and the rest to zero. However, in practice, this proved result in graphs that capture the local structure of the contact maps poorly. This is because intensities follow an exponential distribution with a mean close to zero and some very larges values that correspond t interactions along and close to the main diagonal of the contact maps. Thus, picking relatively large numbers would result in ignoring interactions that are far from the main diagonal and picking small numbers will lead to capturing too many *insignificant* interactions.

In order to threshold the matrix so that both global and local patterns are kept, we borrowed the concept of *adaptive thresholding* from image processing context. In this method, in order to be set, a pixel should have an intensity that is larger than the average of non-zero intensities in its *neighborhood*. The neighborhood is defined by an sliding kernel that passes through the contact map with a pixel at its middle at each step. Figure 1 demonstrates result of this thresholding approach for interchromosomal contact map of chromosome 1. Refer to supplementary material for all 23 interchromosomal thresholding results.

Orbit Extraction

Once the thresholded contact maps are obtained, graphlets and orbits can be extracted. We used the `orca` package in `R` programming language to extract the graphlets. As a result of graphlet extraction, For each loci in each contact map, a *signature vector* of size 73 is created.

We divied the task of graphlet comparison into two parts: first we compare graphlets from each contact map in normal cell lines (MIT) with the same contact maps in the other three Leukemic cells. Second we compare contact maps in a similar way but this time only between leukemic cells. In the former case, the null hypothesis is that there is no difference between contact maps of normal cells and leukemic celss and in the later case, the null hypotheis is that there is no difference between different leukemic cells.

We consider two measures of *difference* when comparing contact map graphlets. The first measure is the distance between signature vectors of a loci in two cell lines. If S_k^A and S_k^B are signature vectors corresponding to loci k in contact

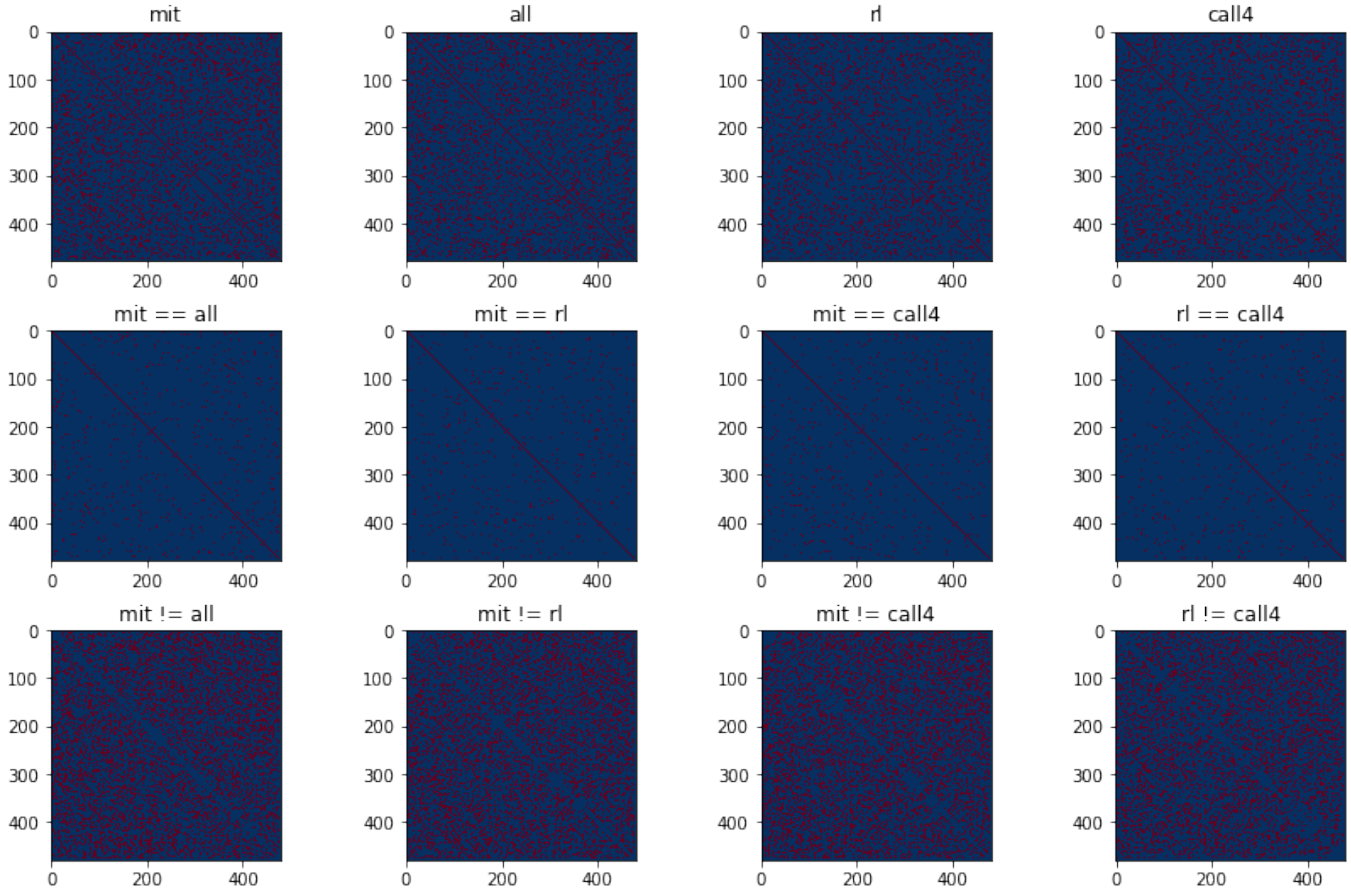

Figure 1. Result of thresholding interchromosomal contact map of chromosome 1 using a kernels of size 5×5. The first row shows the thresholded maps. Second and third rows demonstrate pair-wisesimilarities and differences between contact maps respectively.

maps A and B respectively, then we can caclulate the distance between the two loci using the following formula from (3):

$$d_{ki} = w_i \times \frac{log(S^A_{ki}+1) - log(S^B_{ki}+1)}{log(max(S^A_{ki}, S^B_{ki})+2)} \quad \textbf{(1)}$$

The distance between S and S' can be calculated as follows:

$$D(S^A_k, S^B_k) = \sqrt{\sum_{0}^{72} d^2_{ki}} \quad \textbf{(2)}$$

Using this distance measure, we can quantify how two loci are close to each other in terms of local neighborhood between the two contact maps.

The second measure of comparison that we use captures how similar two orbits are in terms of their frequencies across loci between the two contact maps. For each contact map, we can calculate similarity between orbit distributions by calculating pearso's r correlation. However, pearson's r might not be able to capture non-functional relationships between distributions. As a result, we also used Maximal Information Coefficient (MIC) (7) in order to compare correlations. MIC calculates mutual information (MI) between two distributions, but utilizes dynamic programming in order adjust bin sizes and numbers in order to achieve highest MI. MIC values between two variables fall between 0 and 1, with 0 meaning that the two variables are completely independent and 1 meaning they are totally correlated. We used both Pearson's r and MI in order to compare orbit frequencies. Although results from both approaches were more or less consistent, MIC showed higher robustness than Pearson's r method.

Hypotheses

terminology We denote the set of all contact maps of normal (MIT) cell line with CM. In the same manner we denote CA, CR and CC as the set of all contact maps corresponding to ALL, RL and CALL4 cell lines. We denote a member of any of the aforementioned sets using small letters of the set name. For example, we denote any member of CA with ca.

We denote a contact map by $C^{\{cell_{\{chr1\}\{chr2\}}\}}$, where the superscript denotes the cell type and the subscripts in the superscripts determines the pair of chromosomes the contact map is about. For example $C^{MIT_{1,14}}$ denotes the contact map between chromosomes 1 and 14 in MIT (Normal) dataset. In such a manner $C^{MIT_{1,14}}_{ij}$ denotes the interaction between loci i and j in the aforementioned contact map.

We denote S_i^C as the extracted signature vector of locus i in contact map C. Also P_k^C denotes the frequency distribution of orbital k in contact map C.

With regard to the two aforementioned comparison methods, we define our two null hypotheses as the following:

1. For a locus in a contact map in MIT cell type, its distance from the same locus in the same contact map of the other three cell types are equal to 0.

$$H_0 : D(sm, sa) = 0 \quad \forall cm \in CM \quad \& \quad ca \in CA \tag{3}$$

$$H_0 : D(sm, sr) = 0 \quad \forall cm \in CM \quad \& \quad cr \in CR \tag{4}$$

$$H_0 : D(sm, sc) = 0 \quad \forall cm \in CM \quad \& \quad cc \in CC \tag{5}$$

2. For an orbit extracted from a contact map of MIT cell, the Pearson's r correlation between its frequency and the frequency of the same orbit extracted from the same contact map in the other three cell types in equal to 1.

$$H_0 : Corr(P^C M_k, P^C A_k) = 1 \tag{6}$$

$$H_0 : Corr(P^C M_k, P^C R_k) = 1 \tag{7}$$

$$H_0 : Corr(P^C M_k, P^C C_k) = 1 \tag{8}$$

or

For an orbit extracted from a contact map of MIT cell, the MIC between its frequency and the frequency of the same orbit extracted from the same contact map in the other three cell types in equal to 1.

RESOURCES

Hi-C Datasets:

1. Code base for this article
2. Datasets including cancerous cells
3. Original Datasets

REFERENCES

1. Badri Adhikari, Tuan Trieu, and Jianlin Cheng. Chromosome3d: reconstructing three-dimensional chromosomal structures from hi-c interaction frequency data using distance geometry simulated annealing. *BMC genomics*, 17(1):886, 2016.
2. Erez Lieberman-Aiden, Nynke L Van Berkum, Louise Williams, Maxim Imakaev, Tobias Ragoczy, Agnes Telling, Ido Amit, Bryan R Lajoie, Peter J Sabo, Michael O Dorschner, et al. Comprehensive mapping of long-range interactions reveals folding principles of the human genome. *science*, 326(5950):289–293, 2009.
3. Nataša Pržulj. Biological network comparison using graphlet degree distribution. *Bioinformatics*, 23(2):e177–e183, 2007.
4. Tijana Milenkoviæ and Nataša Pržulj. Uncovering biological network function via graphlet degree signatures. *Cancer informatics*, 6:257, 2008.
5. Tijana Milenković, Vesna Memišević, Anand K Ganesan, and Nataša Pržulj. Systems-level cancer gene identification from protein interaction network topology applied to melanogenesis-related functional genomics data. *Journal of the Royal Society Interface*, 7(44):423–437, 2010.
6. Pietro Di Lena, Piero Fariselli, Luciano Margara, Marco Vassura, and Rita Casadio. Fast overlapping of protein contact maps by alignment of eigenvectors. *Bioinformatics*, 26(18):2250–2258, 2010.
7. David N Reshef, Yakir A Reshef, Hilary K Finucane, Sharon R Grossman, Gilean McVean, Peter J Turnbaugh, Eric S Lander, Michael Mitzenmacher, and Pardis C Sabeti. Detecting novel associations in large data sets. *science*, 334(6062):1518–1524, 2011.